HHS Public Access

Author manuscript

Nat Microbiol. Author manuscript; available in PMC 2017 December 26.

Published in final edited form as:

Nat Microbiol. ; 2: 17099. doi:10.1038/nmicrobiol.2017.99.

Illuminating Vital Surface Molecules of Symbionts in Health and Disease

Jason E. Hudak[1], **David Alvarez**[1], **Ashwin Skelly**[1], **Ulrich H. von Andrian**[1,2], and **Dennis L. Kasper**[1,*]

[1]Department of Microbiology and Immunobiology, Harvard Medical School, Boston, MA 02115, USA

[2]The Ragon Institute of Massachusetts General Hospital, Massachusetts Institute of Technology and Harvard, Cambridge, MA 02139 USA

Abstract

The immunomodulatory surface molecules of commensal and pathogenic bacteria are critical to the microbe's survival and the host's response.[1,2] Recent studies have highlighted the unique and important responses elicited by commensal-derived surface macromolecules;[3–5] however, the technology available to track these molecules in host cells and tissues remains primitive. We report here an interdisciplinary approach that uses metabolic labeling combined with bioorthogonal click chemistry (i.e., reactions performed in living organisms)[6] to specifically tag up to three prominent surface immunomodulatory macromolecules – peptidoglycan (PGN), lipopolysaccharide (LPS), and capsular polysaccharide (CPS) – either simultaneously or individually in live anaerobic commensal bacteria. Importantly, the PGN labeling enables for the first time the specific labeling of live endogenous, anaerobic bacteria within the mammalian host. This approach has allowed us to image and track the path of labeled surface molecules from live, luminal bacteria into specific intestinal immune cells in the living murine host during health and disease. The chemical labeling of three specific macromolecules within a live organism offers the potential for in-depth visualization of host-pathogen interactions.

Current methods to study commensal–host interactions *in situ*, such as fluorescence *in situ* hybridization (FISH) remain limited in scope. Despite significant advances in updating this technology,[7,8] it still suffers from many drawbacks.[9] Chemical-based probes have been utilized to image and track bacterial components that are otherwise recalcitrant to

*All correspondence and material requests should be addressed to Dennis L. Kasper, Dennis_Kasper@hms.harvard.edu.

Data Accessibility Statement

The data that supports the findings of this study are available from the corresponding author upon request including but not limited to raw data, original images, and further technical details.

Author Contributions

J.E.H. designed the experiments, analyzed the data, and wrote the manuscript with help from D.A. and A.S. D.A. provided expertise in two-photon intravital microscopy. D.L.K. supervised the study, edited the manuscript, and provided helpful comments, with assistance from U.H.v.A.

Competing Financial Interests

The authors declare no competing financial interests.

conventional genetic tagging methods.[10,11] Furthermore, the predominantly anaerobic environment of the intestinal lumen presents an additional hurdle to genetically encoded tags such as green fluorescent protein (GFP), which require oxygen to mature. In this vein, we previously reported on a method to tag and trace the CPSs of various live commensal bacteria in cells and animal hosts.[12] This approach utilizes the metabolic incorporation of a non-natural sugar, N-azidoacetylgalactosamine (GalNAz),[13] into bacterial CPS to tag and track the bacterium and its CPS. However, less than 50% of anaerobic microbes tested could be reliably labeled with this approach. Therefore, we sought to expand and improve this method in order to (1) label a larger subset of commensals that did not incorporate GalNAz and (2) extend the tagged targets to other immunomodulatory surface molecules, especially more common bacterial molecules.

For our first target, the PGN component of bacteria seemed an obvious choice as it is a highly conserved structural feature of most bacterial phyla. PGN is sensed by the innate NOD-like receptors in mammalian cells, and the strong link of mutations in these receptors to inflammatory bowel disease (IBD) highlights their importance in maintaining healthy commensal–host interactions.[14,15] The promiscuity of PGN biosynthesis was recently exploited in developing a method to install non-natural fluorescent D-amino acids into bacterial PGN (Fig 1a).[16,17] Since cells use only a defined set of L-amino acids for protein synthesis, only the provided D-amino acids can specifically label the PGN. We wanted to determine whether this approach could be used to label and track anaerobic commensal bacteria both *in vitro* and *in vivo*.

Incubation of anaerobic cultures with the fluorescent D-amino acid hydroxycoumarin amino-D-alanine (HADA) resulted in the successful labeling of a wide range of anaerobic and facultative commensal bacteria, including *Bacteroides fragilis*, *Bacteroides vulgatus*, *Parabacteroides merdae*, *Clostridium clostridioforme*, *Clostridium ramosum*, *Enteroccocus faecalis*, *Escherichia coli*, and *Bifidobacterium adolescentis* (Figs. 1a and 1b, Supplementary Fig. 1a). As a control, we incubated the bacteria with the L-enantiomer of the fluorescent amino acid referred to as HALA which does not incorporate into the PGN or other macromolecules; the minimal background we observed supported the specific labeling of the PGN layer by D-amino acid incorporation. This labeling is both time and concentration dependent, as previously reported (Supplementary Fig. 1b),[16] although overnight incubation with HADA was optimal, as previously reported for labeling with GalNAz.[12]

Given the success of *in vitro* PGN labeling, we examined whether the labeled bacteria could be imaged and traced within the natural niche of the host intestine. *B. adolescentis* and *E. faecalis* were labeled as described and administered to mice via oral gavage and direct intestinal injection, respectively. The bacteria retained the PGN label and were successfully imaged in tissue sections of the small intestine and colon (Fig. 1c, Supplementary Fig. 2a). *E. faecalis* in particular was found close to the tissue in the proximal colon and in the vicinity of $CD11c^+$ antigen-presenting cells (APCs, Fig. 1c). We also synthesized fluorescein-D-lysine (FDL)[16] and labeled *C. clostridioforme* in culture; the imaging of this organism in the murine colon (Supplementary Figs. 2b and 2c) demonstrated the capacity for multicolor labeling.

Since exogenous D-amino acids are not used by mammalian cells,[10] we reasoned that feeding conventionally raised mice the fluorescent D-amino acid might allow selective labeling of endogenous bacteria. Confocal imaging of tissue histology slices from HADA-gavaged specific pathogen–free (SPF) mice showed robust labeling of the commensal bacteria already present in the lumen of the small intestine and the colon 2 h and 4 h, respectively, after gavage (Fig. 1d). By contrast, the HALA-gavaged controls showed little background. This approach overcomes a significant methodologic obstacle by providing the ability to specifically label the endogenous microbiota within a living host.

Further examination of the luminal contents demonstrated that the bacteria in the small intestine were quickly labeled (i.e., within 45 min) after HADA administration, but this signal was washed out within 3 h (Fig. 1e). This result is in accord with previous reports that small-intestinal niches are less populated and rapidly flush luminal content.[18] Correspondingly, the cecum and colon showed maximal labeling of endogenous bacteria within 3–8 h (Fig. 1e). The high signal from HALA samples at earlier time points suggests that several hours are required for the excess label to naturally flush out. Surprisingly, commensal bacteria remained significantly labeled up to 24 h after initial HADA administration by oral gavage (Figs. 1e and 1f, Supplementary Figs. 3a, 3b, and 4). This result suggests that, despite clearance of the PGN label within 6–8 h in rich media *in vitro* (Supplementary Fig. 3c), the label *in vivo* is retained much longer, perhaps because of slow growth rates in the normal gut. Repetition in germ-free (GF) mice showed minimal background signal, again suggesting that the observed fluorescence staining is dependent on PGN from endogenous bacteria (Supplementary Figs. 5a and 5b).

Since our approach labels living bacteria, we also employed multiphoton intravital microscopy to view the dynamics of host–microbiota interaction in real time.[19] Our results showed robust labeling of the commensal microbes in the small and large intestines (Fig. 2a, Supplementary Fig. 6). Videos of these dynamics highlight the ability to view endogenous bacteria moving within the lumen and adhering to the mucosal surface of the epithelial barrier (Supplementary Videos 1 and 2).

If the PGN of HADA-labeled bacteria could be imaged and traced in the lumen, then this approach would have the potential to track PGN from live commensals into specific intestinal cells. Several studies have investigated how free luminal protein or pathogens gain access to gut-associated lymphoid tissue (GALT); however, much less is known about bacterial structural-component transport, especially in commensals.[20,21] Flow cytometry analysis of colonic lamina propria cells from mice receiving HADA or HALA revealed a significant portion of $CD45^+$ lymphocytes containing HADA fluorescence (Fig. 2b, Supplementary Fig. 7). Among these $HADA^+$ lymphocytes, $CD11b^+$phagocytes and $CD19^+$ B cells predominated. This large number of $HADA^+CD19^+$ B cells was a surprise. Although dendritic cells (DCs) are known to stimulate B cells in the GALT,[22] few studies have cited such high levels of direct commensal association with resident B cells.

Aside from $CD19^+$ B cells, the APCs in the $MHCII^+HADA^+$ population of the colon consisted mainly of $CX_3CR1^+CD11c^+CD11b^+$ macrophages and conventional $CD11c^+CD11b^-$ DCs. CX_3CR1^+ macrophages are known to directly sample luminal

bacteria and to play key roles in phagocytosis and antigen presentation in the lamina propria.[21,23] $CD103^+$ cells are the main DCs to migrate to the mesenteric lymph nodes;[21] however, we did not see a significant population of $HADA^+CD103^+$ DCs in the colonic lamina propria (Fig. 2b). This result may be due to the small numbers of this cell type in the lamina propria or may highlight the limited ability of these cells to directly acquire luminal bacteria. To confirm that $HADA^+$ cells did indeed contain PGN or PGN-labeled bacteria, we sorted and imaged the $CD11c^+CX_3CR1^+$ and $CD11c^+CX_3CR1^-$ cells containing HADA fluorescence (Fig. 2c, Supplementary Fig. 8).

Sensing of PGN by the host immune system plays a role in the development and progression of IBD.[14] We used the D-amino acid metabolic labeling approach in a mouse model of colitis to track and image the PGN of commensals during disease-associated inflammation. As seen in Fig. 2d, the mucosal layer within the colon was greatly diminished and this change allowed direct interaction of the labeled endogenous bacteria with the colonic epithelium, a finding previously described in IBD.[24,25] This interaction correlated with an increase in $HADA^+CD45^+$ lymphocytes in the lamina propria (Fig. 2e). Of these lymphocytes, T-cell receptor β (TCRβ)–positive T cells and $CD103^+$ DCs were significantly associated with bacteria/bacterial PGN in the colitic versus healthy host, a finding that further supports a key role for these cells in microbial influences on colitis.[25]

The utility of the PGN D-amino acid labeling approach impelled us to seek yet more surface molecules that could be tagged in order to trace commensals *in vivo*. Recently, an azide-containing 2-keto-3-deoxy-D-mannooctanoic acid (KDO) derivative, 8-azido-8-deoxy-KDO (KDOAz), was shown to incorporate into the LPS of *E. coli* (Supplementary Fig. 9a).[26] Once incorporated, the azido group can be labeled by reaction with a fluorescent strained alkyne to form a stable, covalent triazole.[6] We anticipated that this approach would be broadly applicable since the LPS of many other gram-negative bacteria consists of an acylated lipid A with a KDO linker in its core oligosaccharide.[27] As confirmed by microscopy, flow cytometry, and gel electrophoresis, KDOAz incorporated into LPS and labeled a wide variety of gram-negative intestinal resident bacteria, including *E. coli, Klebsiella, B. vulgatus*, *Bacteroides uniformis*, *Bacteroides eggerthii*, and *Fusobacterium necrophorum* (Supplementary Figs. 9b, 9c, 10).

Thus far, we had successfully shown labeling of CPS, PGN, and LPS on a variety of commensal bacteria. Could we then label all three of these immunomodulatory surface components simultaneously on live commensals and thereby overcome a significant previous obstacle – the simultaneous metabolic labeling of multiple distinct molecules in one organism? Since GalNAz or KDOAz labeling relies on the same azide chemical handle for fluorophore attachment, we devised an orthogonal labeling approach for CPS, using a GalNAc derivative that contains a cyclopropene, N-cyclopropenyl galactosaminyl carbamate (GalCCP), (Fig. 3a).[28] Like azides, cyclopropenes are small and biologically inert functional groups, but they react selectively with tetrazines and at the same time as the azide–alkyne reaction.[29] Thus, LPS and CPS could conceivably be labeled simultaneously with different fluorophores.

We tested our three-component labeling scheme on the commensal *B. vulgatus* since it performed well with the individual components. By flow cytometry and microscopy, we documented distinct labeling of all three components, with minimal background in controls incubated with HALA and GalNAc (Fig. 3b, Supplementary Fig. 11a). The distinct labeling of the LPS and CPS components was confirmed by SDS-PAGE, by which the high-molecular-weight (MW) CPS for tetrazine–GalCCP can be distinguished from the lower-MW LPS ladder for cyclooctyne–KDOAz (Supplementary Fig. 11b).

A main appeal of this approach is its ability to track how individual commensal components are broken down and sensed by immune cells. To test this utility, we incubated three-component-labeled *B. vulgatus* with the murine macrophage cell line J755A.1 or bone marrow–derived macrophages. At early time points, all three components could be seen distinctly in association with phagocytosed bacteria in the macrophages (Figs. 3c and 3d, Supplementary Figs. 12a and 12b). Within 4–24 h, the components were often seen to separate into distinct areas; LPS and CPS were located in large encapsulated endosomes, while the HADA-PGN signal was frequently found in punctate areas around these lysosomal LAMP-1$^+$ compartments (Fig. 3e, indicated by arrowheads). In cells treated with bafilomycin, which halts endosome acidification, these large LPS$^+$CPS$^+$ compartments could not be found; implying this phenomenon is a product of cell-mediated bacterial degradation (Supplementary Fig. 12c).

The three-component-labeled bacteria were also introduced and imaged within the intestinal lumen of the murine host. This experiment was performed (1) on fixed tissue sections from mice given labeled *B. vulgatus* by direct intestinal injection; and (2) with two-photon intravital microscopy on surgically exposed intestinal loops in live mice given labeled *B. vulgatus* by direct application (Figs. 3f and 3g, Supplementary Figs. 13a and 13b). Live videos (Supplementary Videos 3 and 4) highlight the ability to track each component as the bacteria traverse the lumen and interact with host epithelial cells.

The metabolic labeling and click chemistry approach we present here allows, for the first time, simultaneously labeling of three bacterial components: CPS, LPS, and PGN. Since most of the mammalian microbiome resides in the intestine, deciphering how and when these bacterial molecules are obtained by the host is especially important in understanding of the progression of intestinal diseases, including IBD and colorectal cancer.[30] The ability to track these inflammatory (and anti-inflammatory) inducers will enable the study of where they accumulate; which cell types they encounter in GALT; and, ultimately, whether differences in their localization correlate with disease.

Methods

Mice

Male and female 6- to 8-week-old C57BL/6 mice were purchased from Jackson Laboratory. Mice were housed in SPF conditions with food and water *ad libitum*. GF C57BL/6 mice were bred and maintained in sterile vinyl isolators in the animal facility at Harvard Medical School and were provided with sterile food (LabDiets 5K67), water, and bedding. All experiments were conducted in accordance with the guidelines of the U.S. National

Institutes of Health and approved by the Harvard Medical Area Standing Committee on Animals.

Bacteria and growth media

The following bacterial species were used: *Bacteroides fragilis* (NCTC9343), *Bacteroides eggerthii* (DSM 20697), *Bacteroides uniformis* (ATCC8452), *Bacteroides vulgatus* (ATCC8482), *Parabacteroides merdae* (CL03T12C32), *Fusobacterium necrophorum* (AO43), *Clostridium clostridioforme* (2_1_49FAA), *Clostridium ramosum* (AO31), *Escherichia coli* (K12), *Bifidobacterium adolescentis* (L2-32), *Klebsiella* spp. (4_1_44FAA), and *Enterococcus faecalis* (TX0104). All bacteria were grown in a basal peptone-yeast broth containing (per liter) 5 g of yeast extract, 20 g of protease peptone, 5 g of NaCl, 5 mg of hemin, 0.5 mg of vitamin K1, and 5 g of K_2HPO_4. Hemin, vitamin K1, and K_2HPO_4 were added through a filter after the basal medium had been autoclaved. All non-natural metabolites for metabolic labeling were synthesized in-house (see details in Supplementary Note 1).

Metabolic labeling and click chemistry of bacteria

Bacteria were inoculated from a plate culture and grown overnight at 37 °C under anaerobic conditions (80% N_2, 10% H_2, 10% CO_2) in an anaerobic chamber in basal peptone-yeast broth with HADA or HALA (0.8 mM), KDOAz (5 mM), and/or GalCCP (250 μM). Bacteria were pelleted at 5000 × g and washed twice in PBS and once in PBS supplemented with 1% BSA. For the subsequent click reactions with KDOAz and GalCCP, the final pellet was resuspended in one-tenth the original culture volume (e.g., 100 μl for a 1-mL culture) of 1% BSA in PBS with 5 μM DIBAC-Rhod, DIBAC-Cy5, or DIBAC-TAMRA (Click Chemistry Tools) for reaction with azide or 5 μM tetrazine-TAMRA/tetrazine-Cy5 (Click Chemistry Tools) for reaction with GalCCP. The suspension was incubated with agitation for 1 h at 37 ºC, after which the bacteria were pelleted and washed twice with 1% BSA in PBS and once in PBS. For three-component labeling, the bacteria were first reacted with 5 μM DIBAC for 1 h at 37 °C, washed once with PBS, and then reacted with 5 μM tetrazine for 1 h at 37 °C. After the final wash, cells were resuspended in PBS and were administered to mice or fixed in 1% formalin and mounted for microscopy or run on flow cytometry. For monitoring label decay, the bacteria were resuspended in basal broth, and aliquots were removed and fixed in 1% formalin at specified time points.

Tissue culture studies and immunofluorescent microscopy

B. vulgatus was grown overnight in basal peptone-yeast broth with HADA (0.8 mM), KDOAz (5 mM), and GalCCP (250 μM) to an OD_{600} of ~0.6. As a control, bacteria were grown in HALA (0.8 mM) and GalNAc (250 μM). The bacteria were labeled with tetrazine-Cy5 and DIBAC-TAMRA or tetrazine-TAMRA and DIBAC-Rhod as described above. C57BL/6 primary bone marrow–derived macrophages or J775A.1 murine macrophages were isolated from mouse bone marrow or received directly from ATCC respectively without further authentication or mycoplasma testing. 5×10^5 macrophage cells were seeded onto 18-mm coverslips in 12-well plates and grown to confluency under humid conditions in an atmosphere of 5% CO_2 at 37 °C in RPMI medium supplemented with 10% FBS, 1% sodium pyruvate, 1% nonessential amino acids, 1% penicillin–streptomycin, 0.15% sodium

bicarbonate, and 2 mM L-glutamine. Cells were washed with PBS, and each well was filled with RPMI medium containing no penicillin–streptomycin. A 10-μl volume of labeled bacterial cells (MOI ~10) was added to each well and spun at 300 × g for 5 min. For some studies, 0.1 μM bafilomycin (Enzo Life Sciences) was added from a DMSO stock to inhibit lysosome maturation. After incubation for 30 min in 5% CO_2 at 37 °C, the medium was removed, and coverslips were washed with sterile RPMI containing no penicillin–streptomycin and left in RPMI. Coverslips were removed from the plates at 1 h, 4 h, and 24 h; washed with PBS; and fixed for 20 min in 4% paraformaldehyde in PBS. Cells were blocked and permeabilized by incubation with 10% FBA, 1% BSA, and 0.1% Triton X-100 in PBS for 1 h; washed twice with Tris-buffered saline with 0.1% Tween (TBST); and incubated with antibodies to LAMP-1 (sc-19992, clone 1D4B, lot H1612, Santa Cruz Biotechnology) or EEA-1 (sc-6415, clone N-19, lot B1813, Santa Cruz Biotechnology) (1:200 in 2% BSA/PBS) for 16 h (protected from light) at 4 °C. Nuclear staining was performed with acridine orange (Biotium) or DRAQ5 (BioLegend) (1 μg/mL) for 10 min. Coverslips were washed three times with TBST, mounted on glass slides with Mowiol medium, and viewed on an Olympus Fluoview BX50WI inverted confocal microscope. All images were analyzed with Fluoview Viewer Software and prepared in Adobe Photoshop.

Tracking of labeled bacteria in the murine host

For tracking of endogenous bacteria, C57BL/6 mice received 250 μL of 3 mM HADA/HALA in PBS by oral gavage. At specified time points, mice were euthanized with CO_2 and the intestinal tissue and mesenteric lymph nodes were removed. In most experiments, the selected time point was 2 h after gavage for the small intestine and 4 h after gavage for the colon. For tracking of exogenously labeled bacteria, organisms were grown in basal medium containing metabolic labels as described above. Approximately 10^8–10^9 organisms in 100 μL of PBS were directly injected into the lumen of the ileum or proximal colon of live SPF C57BL/6 mice anaesthetized under isofluorane. At 1 h after injection, mice were euthanized with CO_2 and the intestine and mesenteric lymph nodes were removed. In the DSS-induced colitis model, mice received 3% DSS in the drinking water as previously described[31] and were monitored daily. Colonic tissue was collected from mice on day 4 after administration of dextran sodium sulfate (DSS) (i.e., at the onset of intestinal inflammation),[31] and lymphocytes were isolated.

For fluorescence imaging, intestinal tissue was fixed overnight in Carnoy's fixative (60% methanol, 30% chloroform, 10% acetic acid) and submitted to the Harvard Cancer Center Research Pathology Core for paraffin embedding and sectioning. Paraffin was removed by two incubations in xylene substitute (ThermoFisher) for 10 min at 37 °C followed by rehydration with sequential incubation in 100%, 95%, 70%, and 50% ethanol and then in distilled water. Alternatively, tissue was fixed in 4% formalin/DMEM for 4 h at 4 °C, embedded in OCT compound (Tissue-Tek), frozen into tissue molds, and later sectioned at a thickness of ~12 μm with a cryostat. The tissue sections were blocked and permeabilized by incubation with 10% FBA, 1% BSA, and 0.1% Triton X-100 in PBS for 1 h; washed twice with TBST; and incubated with antibodies to CD11c (clone N418, Santa Cruz Biotechnology) or MUC2 (clone H-300, lot F2314, Santa Cruz Biotechnology; 1:200 in 2% BSA/PBS) for 16 h (protected from light) at 4 °C. Secondary antibody to rabbit (AF568-

goat IgG α-rabbit, Life Technologies; 1:1,000 in 2% BSA/PBS) was applied for 1 h at room temperature for MUC2 staining. Nuclear staining was performed with acridine orange (Biotium) or DRAQ5 (BioLegend) (1 μg/mL) for 10 min. Coverslips were washed three times with TBST and mounted on glass slides with Mowiol medium. Confocal images were acquired with an Olympus Fluoview BX50WI inverted confocal microscope. All images were analyzed with Fluoview Viewer Software and prepared in Adobe Photoshop.

For analysis of single-cell isolates, intestinal tissues were cleaned and dissociated as previously described.[32] Intestinal luminal contents were flushed in 5 mL of PBS, and fat was removed from tissue. For analysis of luminal bacteria, the flushed contents were allowed to settle and then filtered through nylon mesh, and material was pelleted and fixed overnight in 1% formalin/DMEM at 4 °C. The cleaned tissue was treated with RPMI containing 1 mM DTT, 2.5 mM EDTA, and 1.5% FBS at 37 °C for 15 min to remove epithelial cells, minced, and dissociated in collagenase solution (collagenase II [Gibco], 1.5 mg/ml ; dispase [Gibco], 0.5 mg/ml; DNAse I [Worthington], 0.05 mg/ml; and 1% FBS in RPMI) with constant stirring at 37 °C for 45 min. Single-cell suspensions were then filtered and washed in 5% FBS RPMI. Cell suspensions were filtered through nylon mesh and resuspended in DMEM without phenol (Gibco/Life Technologies). This process was followed by staining on ice for 20 min (1:200 dilution) with fluorescently labeled antibodies to CD45 (30-F11), CD4 (GK1.5), CD11b (M1/70), CD11c (N418), CD19 (6D5), I-A/I-E (M5/114.15.2), CX_3CR1 (SAO11F11), CD103 (2E7), or TCRβ (H57-597), all from Biolegend. The fixable viability dye eFluor-780 (eBioscience) was used to gate out dead cells. The stained samples were immediately run or fixed in 1% formalin/DMEM overnight and run on flow cytometry (MacsQuant, Miltenyi or LSR-II, BD Biosciences) and analyzed with FlowJo software. Cell suspensions were run on a FACSAria and sorted for $HADA^+$I-A/I-E^+CD11c^+ and further CX_3CR1^+ and CX_3CR1^-.

Intravital two-photon microscopy of the intestine

Intravital two-photon microscopy of mouse intestine was performed as previously described.[12,33] Mice were anesthetized with ketamine-xylazine-acepromazine and positioned on a customized heated stage. A ~2-cm segment of intestine was exteriorized through the peritoneum, immobilized with tissue-adhesive glue and kept hydrated with a mixture of PBS and lubricant gel. Because of the thickness of the intestinal muscularis, the lumen interior was exposed by micro-incision along the intestinal wall followed by careful removal of large fecal matter and mounting on the customized stage. In some preparations, labeled bacteria were injected directly into the intestinal loop otherwise SPF mice were given 3 mM HADA in 250 μl by oral gavage at least 4 h before imaging. For delineation of the intestinal epithelial layer, the exposed luminal section was incubated in wheat germ agglutinin-AF633 (Life Technologies/ThermoFisher; 0.5 mg/ml in PBS) for 10 mins to counterstain before imaging. Two-photon imaging was performed on an Ultima Two-Photon Microscope (Prairie Technologies/Bruker) equipped with a Tsunami Ti:sapphire laser with a 10-W MilleniaXs pump laser (Spectra-Physics) and a 20×/0.95-NA water-immersion objective (Olympus). The two-photon excitation wavelength was set to 815 nm for optimal fluorescence excitation of the HADA coumarin fluorophore while maintaining excitation of additional rhodamine green and TAMRA fluorophores for three-color labeling. Fluorescence

emission was detected with 665/65-nm, 590/50-nm, 525/50-nm, and 450/50-nm bandpass filters for four-color imaging. Raw image sequences were first processed with Volocity software (v6.0; PerkinElmer). Auto-contrasted images were processed with fine noise-reduction filters and each image channel was assigned a pseudo-color according to emitted light wavelengths (bp665/65nm, magenta; bp590/50nm, red; bp525/50nm, green; bp45570nm, blue). For time-lapse videos of the small intestine, processed image sequences were corrected for motion-artifacts uwith ImageJ/Fiji (v2.0.0). Images were motion-corrected by recursive registration of stacks/StackReg[34] with Affine transformation, followed by Elastic Stack Alignment[35] with Rigid transformation.

Statistical analyses

All statistical analyses were performed in Prism (GraphPad Software) and were based on normally distributed data sets with equal variance (Bartlett's test). Gender- and age-matched mice were randomly assigned to groups for *in vivo* experiments. Samples size was chosen for adequate numbers for statistical analyses. Investigators were not blinded during the experiments or outcome assessments. Where applicable, data points are presented as mean ± s.e.m. values unless otherwise stated. Data were inferred as statistically significant if P values were <0.05. The significance of differences between two groups was determined by two-tailed paired Student's t-test.

Supplementary Material

Refer to Web version on PubMed Central for supplementary material.

Acknowledgments

We thank the Harvard Medical School Center for Immune Imaging for providing instrumentation and aid for two-photon microscopy; N. Geva-Zatorsky and F. Gazzaniga for materials, expertise, and helpful discussion; D. Erturk-Hasdemir and N. Okan for aid in cell culture and isolation of bone marrow macrophages; and C. Hudak for helpful discussion and manuscript critique. This work was funded by a grant from the U.S. Department of Defense (W81XWH-15-1-0368) and was supported in part by the U.S. National Institutes of Health (grants PO1 AI1112521, RO1 AI111595 [to U.H.v.A.], and 5T32 HL066987 [to D.A.]). Additional support to U.H.v.A. was provided by the Ragon Institute at MGH, MIT, and Harvard. J.E.H. was supported by the Cancer Research Institute Irvington Fellowship Program.

References

1. Fischbach MA, Segre JA. Signaling in Host-Associated Microbial Communities. Cell. 2016; 164:1288–1300. [PubMed: 26967294]
2. Sommer F, Backhed F. The gut microbiota – masters of host development and physiology. Nat Rev Micro. 2013; 11:227–238.
3. Ayres JS. Cooperative Microbial Tolerance Behaviors in Host-Microbiota Mutualism. Cell. 2016; 165:1323–1331. [PubMed: 27259146]
4. Lebeer S, Vanderleyden J, De Keersmaecker SCJ. Host interactions of probiotic bacterial surface molecules: comparison with commensals and pathogens. Nat Rev Micro. 2010; 8:171–184.
5. Rooks MG, Garrett WS. Gut microbiota, metabolites and host immunity. Nat Rev Immunol. 2016; 16:341–352. [PubMed: 27231050]
6. Sletten EM, Bertozzi CR. Bioorthogonal Chemistry: Fishing for Selectivity in a Sea of Functionality. Angew Chem Int Ed. 2009; 48:6974–6998.
7. Earle KA, et al. Quantitative Imaging of Gut Microbiota Spatial Organization. Cell Host Microbe. 2015; 18:478–488. [PubMed: 26439864]

8. Welch JLM, Rossetti BJ, Rieken CW, Dewhirst FE, Borisy GG. Biogeography of a human oral microbiome at the micron scale. Proc Natl Acad Sci. 2016; 113:E791–E800. [PubMed: 26811460]
9. Moter A, Göbel UB. Fluorescence in situ hybridization (FISH) for direct visualization of microorganisms. J Microbiol Methods. 2000; 41:85–112. [PubMed: 10991623]
10. Siegrist MS, Swarts BM, Fox DM, Lim SA, Bertozzi CR. Illumination of growth, division and secretion by metabolic labeling of the bacterial cell surface. FEMS Microbiol Rev. 2015; 39:184–202. [PubMed: 25725012]
11. Kocaoglu O, Carlson EE. Progress and prospects for small-molecule probes of bacterial imaging. Nat Chem Biol. 2016; 12:472–478. [PubMed: 27315537]
12. Geva-Zatorsky N, et al. In vivo imaging and tracking of host-microbiota interactions via metabolic labeling of gut anaerobic bacteria. Nat Med. 2015; 21:1091–1100. [PubMed: 26280120]
13. Boyce M, Bertozzi CR. Bringing chemistry to life. Nat Methods. 2011; 8:638–642. [PubMed: 21799498]
14. Thaiss CA, Levy M, Suez J, Elinav E. The interplay between the innate immune system and the microbiota. Curr Opin Immunol. 2014; 26:41–48. [PubMed: 24556399]
15. Ogura Y, et al. A frameshift mutation in NOD2 associated with susceptibility to Crohn's disease. Nature. 2001; 411:603–606. [PubMed: 11385577]
16. Kuru E, et al. In Situ Probing of Newly Synthesized Peptidoglycan in Live Bacteria with Fluorescent D-Amino Acids. Angew Chem Int Ed. 2012; 51:12519–12523.
17. Hsu, YP., Meng, X., VanNieuwenhze, MS. Methods in Microbiology. Jensen, CH., Jensen, GJ., editors. Vol. 43. Academic Press; 2016. p. 3-48.
18. Mowat AM, Agace WW. Regional specialization within the intestinal immune system. Nat Rev Immunol. 2014; 14:667–685. [PubMed: 25234148]
19. Helmchen F, Denk W. Deep tissue two-photon microscopy. Nat Methods. 2005; 2:932–940. [PubMed: 16299478]
20. Farache J, et al. Luminal bacteria recruit CD103+ dendritic cells into the intestinal epithelium to sample bacterial antigens for presentation. Immunity. 2013; 38:581–595. [PubMed: 23395676]
21. Mazzini E, Massimiliano L, Penna G, Rescigno M. Oral Tolerance Can Be Established via Gap Junction Transfer of Fed Antigens from CX3CR1+ Macrophages to CD103+ Dendritic Cells. Immunity. 2014; 40:248–261. [PubMed: 24462723]
22. Reboldi A, et al. IgA production requires B cell interaction with subepithelial dendritic cells in Peyer's patches. Science. 2016; 352
23. Diehl GE, et al. Microbiota restricts trafficking of bacteria to mesenteric lymph nodes by CX3CR1hi cells. Nature. 2013; 494:116–120. [PubMed: 23334413]
24. Sánchez de Medina F, Romero-Calvo I, Mascaraque C, Martínez-Augustin O. Intestinal Inflammation and Mucosal Barrier Function. Inflamm Bowel Dis. 2014; 20:2394–2404. [PubMed: 25222662]
25. Sartor RB. Microbial Influences in Inflammatory Bowel Diseases. Gastroenterology. 2008; 134:577–594. [PubMed: 18242222]
26. Dumont A, Malleron A, Awwad M, Dukan S, Vauzeilles B. Click-Mediated Labeling of Bacterial Membranes through Metabolic Modification of the Lipopolysaccharide Inner Core. Angew Chem Int Ed. 2012; 51:3143–3146.
27. Kumada H, Haishima Y, Kondo S, Umemoto T, Hisatsune K. Occurrence of 2-keto-3-deoxyoctonate (KDO) and KDO phosphate in lipopolysaccharides ofBacteriodes species. Curr Microbiol. 1993; 26:239–244.
28. Patterson DM, Jones KA, Prescher JA. Improved cyclopropene reporters for probing protein glycosylation. Mol Biosyst. 2014; 10:1693–1697. [PubMed: 24623192]
29. Patterson DM, Nazarova LA, Xie B, Kamber DN, Prescher JA. Functionalized Cyclopropenes As Bioorthogonal Chemical Reporters. J Am Chem Soc. 2012; 134:18638–18643. [PubMed: 23072583]
30. Elson CO, et al. Experimental models of inflammatory bowel disease reveal innate, adaptive, and regulatory mechanisms of host dialogue with the microbiota. Immunol Rev. 2005; 206:260–276. [PubMed: 16048554]

31. Wirtz S, Neufert C, Weigmann B, Neurath MF. Chemically induced mouse models of intestinal inflammation. Nat Protoc. 2007; 2:541–546. [PubMed: 17406617]

32. Couter CJ, Surana NK. Isolation and Flow Cytometric Characterization of Murine Small Intestinal Lymphocytes. J Vis Exp JoVE. 2016; doi: 10.3791/54114

33. Millet YA, et al. Insights into Vibrio cholerae Intestinal Colonization from Monitoring Fluorescently Labeled Bacteria. PLOS Pathog. 2014; 10:e1004405. [PubMed: 25275396]

34. Thévenaz P, Ruttimann UE, Unser M. A pyramid approach to subpixel registration based on intensity. IEEE Trans Image Process Publ IEEE Signal Process Soc. 1998; 7:27–41.

35. Saalfeld S, Fetter R, Cardona A, Tomancak P. Elastic volume reconstruction from series of ultra-thin microscopy sections. Nat Methods. 2012; 9:717–720. [PubMed: 22688414]

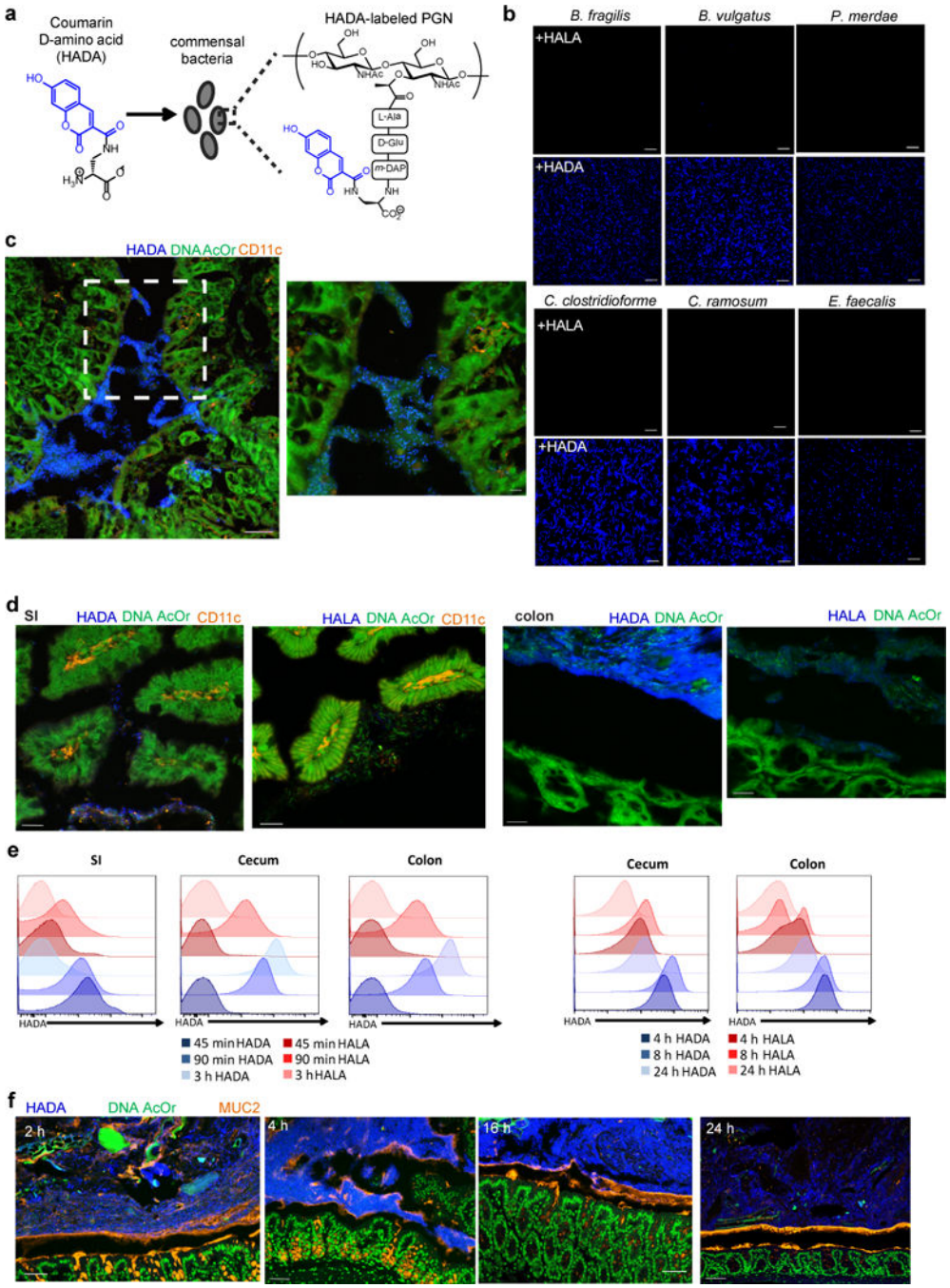

Figure 1. Fluorescent D-amino acid labels PGN in commensal bacteria

(**a**) Schematic of metabolic labeling of the peptidoglycan of commensal bacteria with fluorescent D-amino acid derivatives. The addition of the fluorescent coumarin moiety is highlighted in blue. (**b**) Images of various commensal bacteria grown overnight in medium with a fluorescent amino acid: HADA or (as a negative control) HALA. Scale bars, 10 μm. (**c**) Confocal image and expanded region (right) of frozen, fixed tissue slice of mouse colon 1 h after injection of HADA-labeled *E. faecalis*. AcOr, acridine orange. Scale bar: left, 50 μm; right, 10 μm. (**d**) Confocal images of Carnoy's-fixed, paraffin-embedded tissue slices

from mice 2 h (small intestine [SI], left) or 4 h (colon, right) after oral gavage with HADA or (as a negative control) HALA. Scale bar, 20 μm. (**e**) Flow cytometry histogram plots of luminal contents from mice given HADA or HALA orally demonstrate decay of fluorescent signal over time. (**f**) Confocal images of Carnoy's-fixed, paraffin-embedded tissue slices from mice given HADA orally. The mice were sacrificed, and tissue was fixed at the specified times after oral gavage. The images show significant retention of fluorescent signal over 24 h. MUC2, mucin 2. Scale bar, 50 μm. Data in **c**–**f** are representative of at least three independent experiments.

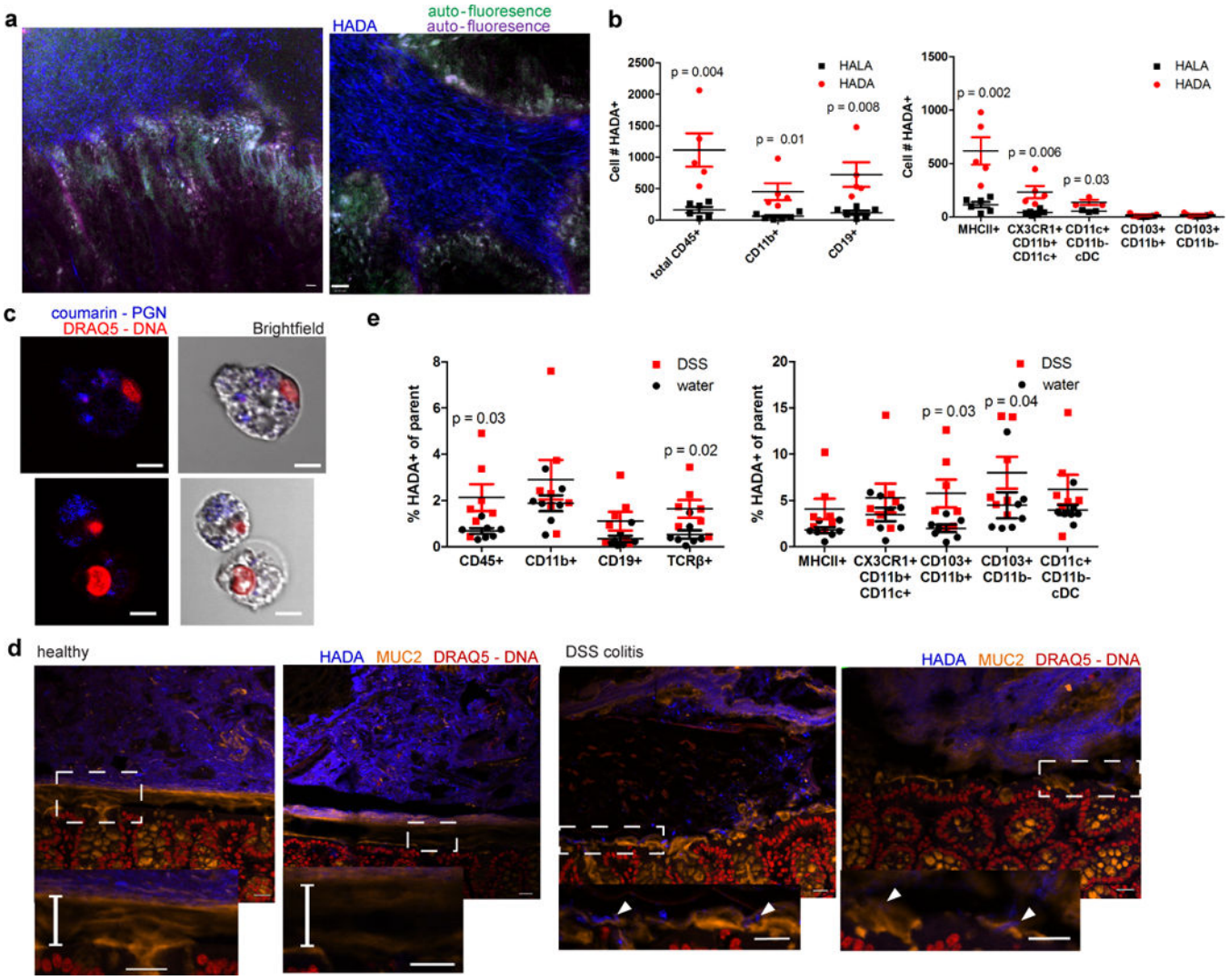

Figure 2. Use of HADA-labeled PGN to track live commensals in the host

(**a**) Representative live images from intravital two-photon microscopy of the murine colon 16 h after administration of HADA. Mice were anesthetized and intestinal loops were surgically extracted and mounted for imaging. Purple and green represent tissue autofluorescence (see Supplementary Videos 1 and 2). Scale bar, 10 μm. (**b**) Numbers of colonic lymphocytes bearing a $HADA^+$ signal 4 h after oral gavage of HADA. Data are mean ± s.e.m. values for biological replicates of n=5 mice (*P* values calculated by paired Student's *t*-test). (**c**) Representative confocal images of live $CD11c^+$ (top) or $CD11c^+CX_3CR1^+$ (bottom) mononuclear phagocytes (sorted for a $HADA^+$ signal) bearing HADA-labeled bacteria/PGN. Scale bar, 5 μm. (**d**) Representative images of Carnoy's-fixed, paraffin-embedded tissue slices obtained 4 h after oral gavage of HADA from mice given normal drinking water (left) or drinking water containing 3% DSS (right) for the preceding 4 days. The damaged mucosal layer and breach with endogenous bacteria are evident in the DSS-induced colitic colons. Bars show mucus thickness is roughly 50 μm in healthy mice while arrows point at bacteria at the epithelial layer in DSS-treated mouse colons. Scale bar, 20 μm. (**e**) Percentages of the parent subpopulation of colonic lymphocytes bearing a

$HADA^+$ signal 4 h after oral gavage with HADA in healthy mice and mice with DSS-induced colitis. Data are mean ± s.e.m. values for biological replicates of n=7 mice (*P* values calculated by paired Student's *t*-test). Data in **a**–**e** are representative of at least three independent experiments.

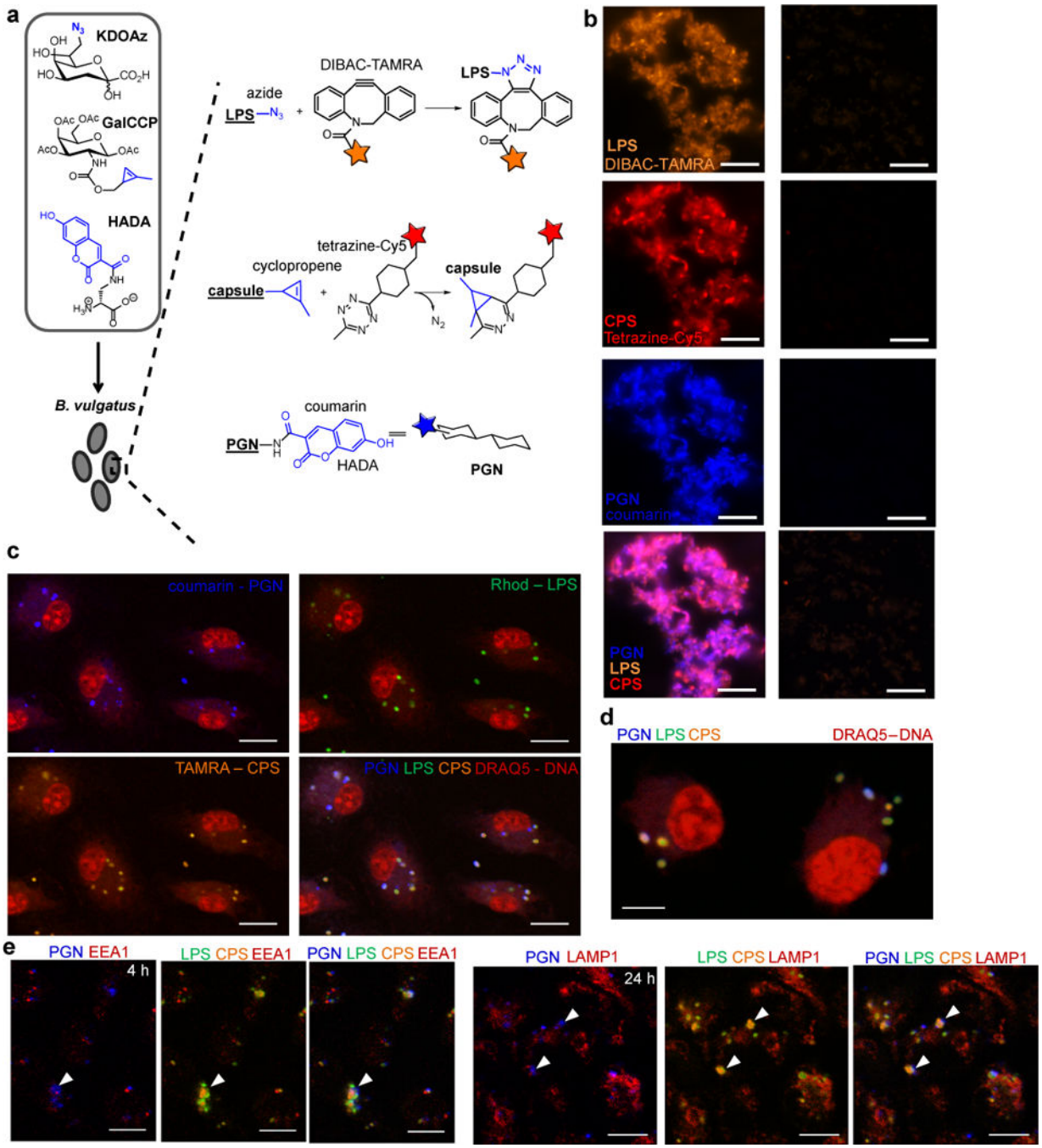

Figure 3. Simultaneous labeling of three cell-surface molecules in commensal bacteria

(**a**) Schematic of the metabolic labeling approach using the non-natural metabolites KDOAz (LPS), GalCCP (CPS), and HADA (PGN) to simultaneously label three cell-surface macromolecules in the commensal bacterium *B. vulgatus*. The reactive or fluorescent moieties are highlighted in blue. DIBAC-TAMRA, dibenzo-aza-cyclooctyne-carboxytetramethylrhodamine; Cy5, cyanine-5. (**b**) Images of *B. vulgatus* grown overnight in medium with KDOAz, GalCCP, and HADA (left) or, as a negative control, with GalNAc and HALA (right) and reacted with DIBAC-TAMRA and tetrazine-Cy5. Scale bar, 10 μm.

(**c**) Confocal images of fixed bone marrow–derived macrophages 1 h after inoculation of three-component-labeled *B. vulgatus*. Rhod, rhodamine green; DRAQ5, red DNA dye. Scale bar, 5 μm. (**d**) Zoomed confocal image of bone marrow–derived macrophages bearing three-component-labeled *B. vulgatus.* Scale bar, 5 μm. (**e**) Representative images of J775A.1 murine macrophages 4 h and 24 h after inoculation of three-component-labeled *B. vulgatus*. Arrows highlight where PGN is seen separate from colocalized CPS/LPS. Scale bar, 10 μm. Data in **b**–**e** are representative of at least three independent experiments with n=3 technical replicates.

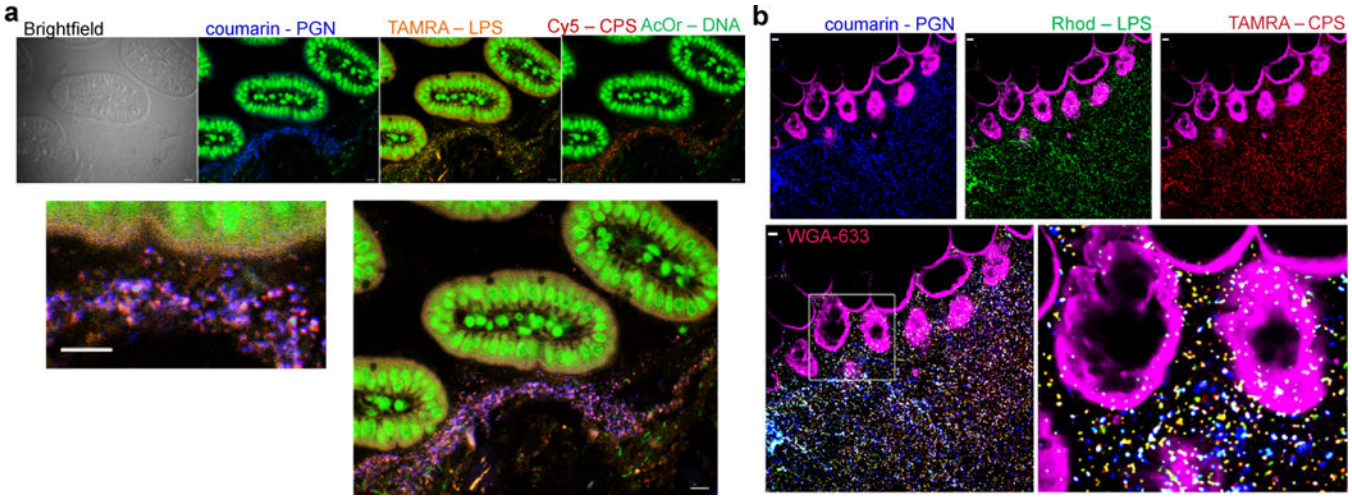

Figure 4. Simultaneous labeling of three cell-surface molecules in commensal bacteria

(**a**) Confocal image of Carnoy's-fixed, paraffin-embedded tissue slices obtained from mice 1 h after intestinal injection of labeled *B. vulgatus*. Zoomed image (lower left) is shown to highlight interaction with the host epithelial layer. Scale bar, 10 μm. (**b**) Representative live images from intravital two-photon microscopy of the murine small intestine after direct inoculation with three-component-labeled *B. vulgatus*. Purple represents lectin staining of the epithelium with WGA-633 (see Supplementary Videos 3 and 4). Scale bar, 10 μm. Data are representative of at least three independent experiments with n = 3 mice per experiment.